Published in final edited form as:
Cell Host Microbe. 2013 November 13; 14(5): . doi:10.1016/j.chom.2013.10.012.

HIV-1 induces the formation of stable microtubules to enhance early infection

Yosef Sabo[1], **Derek Walsh**[2], **Denis S. Barry**[3,#], **Sedef Tinaztepe**[1,4], **Kenia de los Santos**[1], **Stephen P. Goff**[1], **Gregg G. Gundersen**[5], and **Mojgan H. Naghavi**[1,3,*]

[1]Department of Biochemistry and Molecular Biophysics, Howard Hughes Medical Institute, Columbia University, New York, NY 10032, USA. [2]Department of Microbiology, New York University School of Medicine, New York, NY 10016, USA. [3]Centre for Research in Infectious Diseases, University College Dublin, Dublin 4, Ireland. [4]Department of Genetics and Development, Columbia University, New York, NY 10032, USA. [5]Department of Pathology and Cell Biology, Columbia University, New York, NY 10032, USA.

Summary

Stable microtubule (MT) subsets form distinct networks from dynamic MTs and acquire distinguishing posttranslational modifications, notably detyrosination and acetylation. Acting as specialized tracks for vesicle and macromolecular transport, their formation is regulated by the end-binding protein, EB1, which recruits proteins that stabilize MTs. We show that HIV-1 induces the formation of acetylated and detyrosinated stable MTs early in infection. Although the MT depolymerizing agent nocodazole affected dynamic MTs, HIV-1 particles localized to nocodazole-resistant stable MTs and infection was minimally affected. EB1 depletion or expression of an EB1 carboxy-terminal fragment that acts as a dominant negative inhibitor of MT stabilization, prevented HIV-1-induced stable MT formation and suppressed early viral infection. Furthermore, we show that the HIV-1 matrix protein targets the EB1-binding protein, Kif4 to induce MT stabilization. Our findings illustrate how specialized MT-binding proteins mediate MT stabilization by HIV-1 and the importance of stable MT subsets in viral infection.

Introduction

Long-range intracellular transport involves directed cargo movement by motor proteins on microtubules (MTs) (Dodding and Way, 2011). MTs are composed of α-/β-tubulin heteropolymers that form polarized filaments whose minus-ends are anchored at the perinuclear MT-organizing center (MTOC) while their more dynamic plus-ends extend toward the plasma membrane (Li and Gundersen, 2008). Although MTs in many cell types are highly dynamic, exploring the intracellular environment through “search and capture”, subsets of MTs are highly stable. Stable MTs acquire distinguishing posttranslational modifications including detyrosination and acetylation, and are recognized by specific motor proteins to act as specialized tracks for vesicle trafficking (Janke and Bulinski, 2011). As

[*]**Corresponding author:**mn2034@columbia.edu, Phone: 212-305-7956, Fax: 212-305-5106.
[#]Present Address: Department of Anatomy and Neuroscience, University College Cork, Ireland.

detyrosination exposes a glutamic acid at the carboxy-terminus of tubulin these subsets are also known as Glu-MTs. MT stabilization is regulated by MT plus-end tracking proteins (+TIPs) that are recruited to dynamic MT ends by the end-binding protein, EB1 (Gouveia and Akhmanova, 2010). +TIPs interact with a range of proteins, including cortical actin to link MTs to the cell cortex, while localized signaling controls +TIP function thereby inducing MT stabilization at specific sub-cellular sites (Janke and Bulinski, 2011; Li and Gundersen, 2008).

Viruses have evolved a variety of strategies to hijack cytoskeletal networks to facilitate their movement (Dodding and Way, 2011). Retroviruses use actin microfilaments for short-range transport at the cell periphery and MT motors for long-range intracellular movement (Campbell and Hope, 2005; Naghavi and Goff, 2007). Although little is known about early post-entry trafficking of retroviral cores, the HIV-1 reverse transcription complex (RTC) interacts with both actin and MT cytoskeletons (Bukrinskaya et al., 1998; Contreras et al., 2012; McDonald et al., 2002), suggesting that viral proteins function in early actin-mediated movement and the transition of viral cores to the MT network. Retroviral particles move in a dynein-dependent manner along MTs to the nucleus, with uncoating and RT thought to occur during MT-dependent trafficking or upon reaching the nucleus (Arhel et al., 2006; Arhel et al., 2007; McDonald et al., 2002; Petit et al., 2003; Su et al., 2010). While numerous screens have identified cytoskeletal factors as regulators of infection, our recent screens specifically identified regulators of MT stability (Haedicke et al., 2008; Henning et al., 2011; Naghavi et al., 2007). However, these factors are broad regulators of both actin and MT organization and, as such, our understanding of the specific contribution of stable MTs to infection remains limited.

Here we show that HIV-1 induces MT stabilization early in infection of a number of human cell types. Incoming viral particles associated with stable MTs even in the presence of nocodazole, suggesting an underappreciated role for these MT subsets in early infection. By depleting EB1 or expressing a dominant negative inhibitor of +TIP recruitment to EB1, we show that EB1 promotes HIV-1 infection after fusion of viral cores into the cytoplasm through effects on stable MTs. In EB1-depleted cells HIV-1 particles failed to reach the nucleus. Finally, we demonstrate that HIV-1 matrix (MA), a component of incoming viral particles and of the Gag polyprotein, targets the EB1-binding protein, Kif4 to induce MT stabilization. Our findings illustrate how HIV-1 has evolved to target specialized +TIPs to control MT stability and promote early post-entry stages of infection.

Results

HIV-1 infection induces MT stabilization

To determine whether HIV-1 affects MT stability cells were infected with viruses carrying HIV-1 envelope or either of two independent envelopes widely used for pseudotyped infection. Cells were fixed at various times in hours post-infection (h.p.i.) and stained for tyrosinated (Tyr-MTs) or acetylated (AC-MTs) tubulin. While no detectable differences in Tyr-MTs were observed between uninfected and infected samples, immunofluorescence (IF) demonstrated that HIV-1 carrying wt envelope induced AC-MT formation in U87.CD4.CCR5 cells (Figure 1A). To test whether this was cell type-dependent or envelope-dependent, different cell types were mock infected or infected with HIV-1 pseudotyped with vesicular stomatitis virus G envelope glycoprotein (HIV-1-VSV). IF analysis demonstrated that HIV-1 induced AC-MT formation in primary normal human dermal fibroblasts (NHDFs) (Figure 1B) and 293A cells (Figure S1A), as well as in natural target cell types, human microglia (CHME3) and primary human macrophages (Figure 1 C-D). This was confirmed by quantification of fluorescence intensity of AC-MTs (Figure S1B-E) or by determining the percentage of AC-MT positive cells (Figure S1F). Furthermore,

although IF analysis in T-cells is complicated by their small cytoplasm, AC-MT induction by HIV-1 was readily detected by western blot (WB) analysis of mock infected or infected Jurkat cells, a human T cell lymphoblast-like cell line (Figure 1E) as well as primary human macrophages (Figure 1F). Heat-inactivated virus (Figure S1G and S1H) or viruses lacking envelope glycoproteins that cannot enter cells (Figure S1I and S1J) did not induce AC-MTs. As viral particles without envelope cannot be titered, WB analysis of Gag protein levels was used to normalize amounts of enveloped and non-enveloped virions used for infections (Figure S1K). Finally, IF analysis showed that HIV-1 also induced the formation of detyrosinated MTs (Figure S1L) and WB analysis confirmed increases in both AC- and Glu-MTs in HIV-1-infected samples (Figure S1M and S1N). The acquisition of both modifications demonstrated that HIV-1 induced MT stabilization rather than a singular tubulin modification, and further evidence of MT stabilization is presented below. Differences in the kinetics of induction matched known differences in the kinetics of entry mediated by different envelope glycoproteins (Hulme et al., 2011), suggesting that it occurred post-entry.

HIV-1 enters the cell by either membrane fusion or endocytosis (Miyauchi et al., 2009). Pseudotyping allows these distinct routes to be tested. HIV-1-VSV, used above, enters the cell by endocytosis. To further confirm that MT stabilization was envelope-independent, murine leukemia virus (MuLV) amphotropic envelope, which induces fusion at the cell surface, was used to pseudotype HIV-1 (HIV-1-Ampho). Similar to HIV-1 and HIV-1-VSV, HIV-1-Ampho induced MT stabilization in various human cells (Figure S1O-T). MT stabilization by HIV-1-Ampho was delayed compared with HIV-1-VSV, consistent with the kinetics of entry by fusion at the cell surface being slower than entry via the endocytic pathway (Hulme et al., 2011). These findings showed that HIV-1 induced MT stabilization in different human cell types regardless of the viral envelope and entry pathway starting as early as 1-2h.p.i.

Nocodazole does not disrupt stable MTs and only moderately reduces HIV-1 infection

The MT depolymerizing agent nocodazole has been reported to exert only small effects on various stages of HIV-1 infection (Jouvenet et al., 2006; Yoder et al., 2011). However, stable MTs are highly resistant to nocodazole and, as such, their importance to infection may be underestimated. To test this, the effects of nocodazole on infectivity and MT organization were examined. For infection, cultures were treated for 1 h with 0.1-10 μM nocodazole, spanning the range used in previous studies, then infected with HIV-1-VSV or HIV-1-Ampho in the presence of nocodazole. In line with previous reports, nocodazole only moderately reduced infection of two different cell types by pseudotyped viruses that enter the cell by distinct routes (Figure 2A-2D). Although dynamic Tyr-MTs were depolymerized at 0.1-1 μM nocodazole, significant levels of stable AC-MTs persisted even at the highest concentrations tested (Figures 2E and 2F). While the modest reduction in HIV-1 infection caused by nocodazole correlated with depolymerization of dynamic MTs, nocodazole-resistant stable MTs could explain the relatively high levels of infectivity that persist in treated cells.

We next examined whether incoming virions localize to stable MTs by infecting CHME3 cells with HIV-1-VSV carrying GFP-tagged Vpr (McDonald et al., 2002). Titration of our virus preparations for p24 content by WB analysis suggests that the particle-to-pfu ratio was typically in the range of 1,000:1; thus, infecting cells at a multiplicity of ~1 represents the addition of about 1,000 physical particles. While only a small fraction of the applied virions mediate all steps required for successful infection, we image all of them. Fixed samples were stained for GFP, Tyr and AC-MTs and then imaged using confocal microscopy. IF analysis revealed that viral particles localized to AC-MT networks in infected cells (Figure 3A). Co-staining for HIV-1 p24 revealed that GFP-Vpr-positive particles represented virus

at various stages of infection (Figure 3B); at the 2h point tested many were still in early stages and exhibit co-localization with p24, while p24 is lost from viral particles that have uncoated (Hulme et al., 2011). p24 puncta that did not stain for GFP-Vpr likely represent natural subpopulations of virus that do not acquire significant amounts of the GFP-Vpr marker. Quantification of the number of viral particles on AC-MTs revealed that ~20% were associated with stable MTs by 1h.p.i. as viral particles began entering the cell and reached ~50% by 2h.p.i. and ~90% by 4h.p.i (Figure 3C). The kinetics with which the percentage of viral particles associated with AC-MTs increased was similar to the kinetics of AC-MT induction by HIV-1 (Figure 1), suggesting that incoming viral particles induce and associate with stable MTs. Finally, to test whether stable MTs might contribute to HIV-1's relative insensitivity to nocodazole, CHME3 cells were treated for 20 min with nocodazole and then infected with HIV-1-VSV-GFP-Vpr. While nocodazole disrupted dynamic MTs (Figure 2F and 3D), IF analysis showed that HIV-1 particles continued to localize to AC-MTs in treated cells (Figure 3D). These findings showed that while dynamic MTs support a modest level of infection, HIV-1 induces and associates with stable MT subsets early in infection and in nocodazole-treated cells.

EB1 is required for HIV-1 induced MT stabilization and viral infection

EB1 is a central regulator of both MT dynamics and stabilization (Gouveia and Akhmanova, 2010). To determine whether it was required for HIV-1-induced MT stabilization, siRNAs were used to deplete EB1 in NHDFs prior to infection. IF analysis showed that in control siRNA-treated cultures HIV-1 induced AC-MTs at 2h and 6h.p.i., and this induction was blocked by EB1 depletion (Figure 4A-B and S2). To determine the impact of preventing EB1-mediated MT stabilization on infection, siRNA-treated cultures were infected with luciferase reporter viruses. Luciferase assays revealed that compared to control siRNA-treated cultures, EB1 depletion using either of two independent siRNAs potently reduced infection by HIV-1-VSV or HIV-1-Ampho in both NHDFs (Figure 4C and 4D) and CHME3 cells (Figure 4F), demonstrating that effects were independent of the viral entry pathway. Furthermore, WB (Figure 4E and 4H) and quantitative PCR (Figure 4G) analysis showed that effects on infection correlated with the levels of EB1 depletion achieved with each siRNA. We have observed that Jurkat T-cells express very high levels of EB1 and contain high levels of AC-MTs compared with other cell types tested. However, even partial depletion of EB1 detectably reduced AC-MTs levels and resulted in a corresponding decrease in HIV-1 infection (Figure 4I and 4J). This demonstrated that EB1 is a critical regulator of MT stabilization and infection by HIV-1 in several cell types.

EB1 influences HIV-1 infection through its effects on stable MTs

To further test the role of MT stabilization we generated a human version of a previously described carboxy-terminal fragment of mouse EB1 (EB1-C) (Wen et al., 2004). EB1-C contains the C-terminal region that binds +TIPs but lacks the N-terminal MT binding domain. As such, EB1-C does not interfere with dynamic MTs but binds +TIPs and competitively blocks their recruitment to endogenous EB1, thereby acting as a dominant negative inhibitor of MT stabilization (Wen et al., 2004). CHME3 lines expressing Flag-tagged human EB1 (EB1-Flag), Flag-tagged EB1-C (EB1-C-Flag) or Flag alone were generated. WB analysis using anti-Flag antibody confirmed the expression of EB1-Flag and EB1-C-Flag in two independent clones (Figure 5A). To determine expression levels of exogenous forms of EB1 relative to endogenous EB1, we used anti-EB1 antibody (Figure 5A). EB1-Flag exhibited reduced mobility in SDS-PAGE and was expressed to levels at or above those of endogenous EB1. EB1-C-Flag could not be detected using anti-EB1 antibody as it lacks the target epitope. However, anti-Flag WB indicated that the level of EB1-C-Flag expression was significantly lower than that of EB1-Flag and, as such, was significantly lower than that of endogenous EB1. To determine the effects of EB1-Flag and EB1-C-Flag

on MT stabilization by HIV-1 these lines were infected, fixed and stained for Tyr- and AC-MTs. AC-MTs were increased in a Flag clone infected with HIV-1-VSV or HIV-1-Ampho and a more pronounced increase occurred in a clone expressing EB1-Flag (Figure 5B and 5C), demonstrating that EB1 facilitated HIV-1-induced MT stabilization. By contrast, HIV-1-induced stable MT formation was partially suppressed in a clone expressing EB1-C-Flag compared to both Flag-expressing and EB1-Flag clones (Figure 5B and 5C). The relatively low efficiency with which EB1-C-Flag reduced stable MT induction compared to Flag-expressing lines reflects the fact that high-level expression over endogenous EB1 could not be achieved, limiting its efficacy as a dominant-negative. Regardless, these findings showed that the expression of exogenous EB1 or EB1-C was sufficient to modulate stable MT levels in infected cells.

To determine effects on infection, these clones were infected with HIV-1-VSV or HIV-1-Ampho reporters. While both EB1-Flag lines showed a significant increase in infection compared to the Flag line, both EB1-C-Flag clones exhibited reduced infection below levels of the control Flag line (Figure 5D and 5E). WB analysis confirmed that EB1-Flag expression enhanced stable MT levels in these lines and increased infection, while EB1-C-Flag reduced stable MT levels and reduced infection (Figure 5D and 5E). Again, effects of EB1-C on viral infection were partial, in line with modest reductions in stable MT levels in EB1-C-expressing lines. However, this demonstrated that even modest changes in stable MT levels affected HIV-1 infection.

EB1 promotes an early post-fusion stage of HIV-1 infection

To determine the point in the viral lifecycle affected by EB1, CHME3 cells were treated with control or EB1 siRNAs. Cultures were then infected with HIV-1-VSV and levels of minus strand strong stop (MSS) DNA, the first detectable retroviral DNA, as well as total viral DNA were determined (Henning et al., 2010). WB analysis confirmed EB1 depletion by targeting siRNAs and the resulting reduction in Glu- and AC-MTs (Figure 6A). Quantitative real-time PCR (qPCR) analysis of viral MSS DNA (Figure 6B) and total viral DNA (Figure 6C) showed that EB1 depletion potently inhibited infection before or at the initiation of RT and viral DNA synthesis. While envelope-independent effects on viral infection suggested that EB1 affected post-entry stages of infection, to test this we used a previously described fusion assay in which HIV-1 cores containing a β-lactamase-Vpr fusion protein allows monitoring of viral penetration into the cytosol (Cavrois et al., 2002). Fusion assays in EB1-Flag and EB1-C-Flag clones (Figure 6D and E) as well as EB1-depleted NHDFs (Figure 6F) showed that EB1 did not notably affect fusion of HIV-1 into the cytoplasm. To explore this further, NHDFs were treated with control or EB1 siRNAs and then infected with HIV-1-VSV-GFP-Vpr. Because EB1 depletion prevents stable MT formation, samples were fixed and stained for Tyr-MTs to visualize MT organization and cell shape, and GFP to detect viral particles. Confocal microscopy revealed that at 1h.p.i. viral particles localized to MTs at the cell periphery in both control and EB1-depeleted cells (Figure 6G). However, by 4h.p.i. viral particles were accumulating near the nucleus in control siRNA-treated samples but remained near the cell periphery and distant from the nucleus in EB1-depleted cells. These effects were quantified in samples taken at 1, 2 and 4h.p.i. by measuring the distance of viral particles from the nucleus in acquired *z*-stacks, excluding the rim of the cell to ensure that virus had entered (Figure 6H). Data is presented as the percentage of total viral particles within the cell that are within 2μm of the nucleus. Results showed that control and EB1-depleted cells were indistinguishable at 1h.p.i., with low percentages likely reflecting small numbers of particles entering the cell at regions of the plasma membrane proximal to the nucleus. By 2-4h.p.i. the number of viral particles within 2μm of the nucleus increased in control samples while this was potently inhibited by EB1 depletion (Figure 6H). IF analysis confirmed the efficacy of EB1 depletion and that this

blocked AC-MT induction in these assays (Figure S3A B). This suggested that EB1-mediated MT stabilization was required for efficient translocation of viral particles across the cytoplasm.

Kif4 mediates MT stabilization and early infection by HIV-1

EB1 regulates MT stabilization by recruiting +TIPs to MT ends. We recently identified the kinesin Kif4 as an EB1-binding protein that induces MT stabilization in mouse cells (Morris et al. (Gundersen, submitted). siRNA-mediated depletion of Kif4 in 293A cells or NHDFs confirmed that Kif4 also regulated MT stability in human cells (Figure 7A). To determine whether Kif4 localized to the ends of stable MTs in HIV-1-infected cells, 293A or CHME3 cells were infected with HIV-1-VSV. Cultures were fixed, stained for Kif4 and Glu-MTs and then analyzed by Total Internal Reflection Fluorescence (TIRF) microscopy to image MTs at the cell periphery. TIRF microscopy revealed that Glu-MT ends were decorated with Kif4 puncta (Figure 7B-C), suggesting that Kif4 could facilitate MT stabilization in infected cells.

Previously Kif4 was found in a yeast two-hybrid library screen to interact with the retroviral Gag polyprotein (Kim et al., 1998; Tang et al., 1999), and the binding site for Kif4 in Gag has been mapped to MA (Tang et al., 1999). To test whether Gag or MA affect MT stability, CHME3 cells or NHDFs were transfected with control plasmid or plasmids expressing HIV-1 Gag or MA. WB analysis showed that expression of either viral protein resulted in the accumulation of AC-MTs (Figure 7D). AC-MTs were also increased by expression of MA from Simian Immunodeficiency Virus (SIV) (Figure S4A), demonstrating that this was not a property unique to HIV-1 MA. Thus, stable MTs could be induced not only by introduction of virus proteins by infection, but also by expression of Gag or MA after transfection. This latter approach allowed us to test whether MA binding to Kif4 mediated MT acetylation as mutations in MA affect viral particle formation preventing us from determining its role in how incoming virions induce AC-MTs. To do this, we tested the effect of MA mutants in the context of the Gag polyprotein. HeLa cells were transfected with HA-tagged forms of Gag followed by co immunoprecipitation (Co-IP) with anti-Kif4 antibody. While wt Gag as well as Gag variants with mutations in the N-terminal myristoylation site or lacking amino acids 112-131 in the C-terminal region of MA bound Kif4 and induced AC-MTs, deletion of amino acids 32-51 in the N-terminus of MA impaired both Gag's interaction with Kif4 and its ability to induce MT acetylation (Figure 7E and 7F). This demonstrated that MA mediated targeting of Kif4 by Gag to regulate MT stability, and suggested that MA in incoming viral particles could explain the ability of HIV-1 to induce MT stabilization early in infection. To test this, Kif4 was depleted in NHDFs or CHME3 cells and cultures were infected with HIV-1-VSV. IF analysis revealed that Kif4 depletion suppressed AC-MT induction by HIV-1 (Figure 7G and S4B). Finally, depletion of Kif4 inhibited early infection with HIV-1-VSV or HIV-1-Ampho as determined by effects on luciferase reporter gene expression (Figure 7H and 7I, respectively) and qPCR analysis of viral MSS DNA (Figure 7J) and total viral DNA (Figure 7K) levels. As such, like EB1, depletion of Kif4 blocked stable MT formation and early stages of infection before or at the initiation of RT and viral DNA synthesis.

Discussion

Although MTs typically form highly dynamic networks, recent work has highlighted the biological importance of stable MT subsets to processes such as cell polarization, differentiation and motility. However, the potential importance and regulation of these specialized MT networks during viral infection remains poorly understood. Here we show that HIV-1 rapidly induces the formation of post-translationally modified stable MTs and

identify key roles for EB1 and its binding partner, Kif4 in regulating MT stability and early post-entry stages of infection.

HIV-1 associates with MTs soon after fusion of viral cores into the cytoplasm and travels to the nucleus in a dynein-dependent manner (Arhel et al., 2006; McDonald et al., 2002). Perhaps paradoxically given the limitations to free diffusion in the cytoplasm, observations that nocodazole has little effect on various stages of HIV-1 infection have led to suggestions that MTs do not play an important role in retroviral infection (Jouvenet et al., 2006; Yoder et al., 2011). However, one study speculated that this might be due to nocodazole-resistant MTs, although this was not tested (McDonald et al., 2002). Here we show that stable MTs persist in nocodazole-treated cells and that viral particles localize to these MT subsets. This suggests that HIV-1 can utilize stable MTs early in infection and that studies using nocodazole underestimate their importance to infection. Indeed, indirect lines of evidence support this; the cytoskeletal cross-linking factors Ezrin and Moesin negatively regulate stable MTs and suppress retroviral infection (Haedicke et al., 2008; Naghavi et al., 2007). However, these factors also influence other cellular functions, including actin organization. Furthermore, histone deacetylase 6 (HDAC6) deacetylates tubulin and suppresses infection by HIV-1 (Valenzuela-Fernandez et al., 2005). However, the direct contribution of MT acetylation to these effects remains unknown as HDAC6 regulates many other host functions. Using both RNAi and dominant negative approaches to block EB1-mediated MT stabilization, we demonstrate the functional importance of stable MTs to HIV-1 infection. Depleting EB1 prevented HIV-1-induced MT stabilization and potently inhibited early infection. Although we could not achieve levels of EB1-C expression that exceeded endogenous EB1 to potently exert a dominant negative effect, even the modest reductions in stable MT levels accomplished with this approach resulted in a corresponding decrease in viral infection. This sharply contrasts with the effects of nocodazole wherein potent depolymerization of dynamic MTs has limited effects on infection. Depletion of EB1 blocked infection after viral fusion but before or at viral DNA synthesis. A number of actin-MT linking factors (Haedicke et al., 2008; Henning et al., 2010; Leung et al., 2006; Naghavi et al., 2007) and MT-associated proteins (Gallo and Hope, 2012) affect a similar post-fusion early stage in retroviral infection. As such, the onset of viral DNA synthesis after entry of HIV-1 into the cell seems to be intricately linked to the transition of viral particles from actin to MTs. Indeed, RT is thought to occur during MT-dependent trafficking to the nucleus (Arhel et al., 2006; Arhel et al., 2007; McDonald et al., 2002; Petit et al., 2003; Su et al., 2010). Our findings that EB1 depletion blocks MT stabilization and inhibits the translocation of HIV-1 particles through the cytoplasm to the nucleus and blocks RT supports this model, and further suggests that stable MTs are particularly important to these early stages of infection.

Stable MTs have long half-lives and are recognized by specific motor proteins to act as specialized tracks for cargo trafficking (Janke and Bulinski, 2011; Li and Gundersen, 2008). These properties make them potentially ideal targets for viruses to reach their intracellular sites of replication. Indeed, a number of viruses induce tubulin acetylation yet whether this represents MT stabilization in each case, the underlying mechanism of induction and the contribution to infection remains unclear (Elliott and O'Hare, 1998; Frampton et al., 2010; Husain and Harrod, 2011; Jouvenet et al., 2004; Kannan et al., 2009; Naranatt et al., 2005; Parker et al., 2002; Warren and Cassimeris, 2007; Yea et al., 2007). Kaposi's sarcoma-associated herpesvirus (KSHV) induces MT acetylation within 30 minutes of infection through integrin-mediated activation of signaling pathways (Naranatt et al., 2005). Here we show that HIV-1 rapidly induces MT stabilization as demonstrated by the accumulation of two post-translational modifications, acetylation and detyrosination, which serve as distinct markers for MT stabilization. Stabilization occurred independently of the envelope used or route of viral entry, while the kinetics of induction by viruses pseudotyped with different

envelopes matched the kinetics of viral entry mediated by these envelopes (Arhel et al., 2006; Hulme et al., 2011; McDonald et al., 2002). This suggests that stabilization occurred early after viral entry. In line with this, MT stabilization was induced by exogenous expression of the viral structural polyprotein Gag or the processed Gag subunit, MA, present in incoming particles. Gag and MA bind the kinesin Kif4 (Kim et al., 1998; Tang et al., 1999). We have found that Kif4 acts as a MT stabilizing factor and demonstrate that an N-terminal region of MA mediates binding of Gag to Kif4 and efficient AC-MT induction. Furthermore, we show that Kif4 is required for incoming viral particles to stabilize MTs and for early stages of viral infection. It is notable that MT stabilization is regulated at localized sites at the cell periphery (Li and Gundersen, 2008). The low-level induction of AC-MTs detected by both WB and IF at 1-2 h.p.i. suggests a model whereby MA present in incoming virions triggers localized MT stabilization at or near the site of virus entry to facilitate very early stages of infection. Although m.o.i.s ranging from 1-3 were used in our studies, our virus preparations typically have particle-to-pfu ratios in the range of 1000, and so infected cells are exposed to many more physical particles. Many of these will enter cells and contribute to the initial MT stabilization detected very early in infection. The continued increase in MT stabilization as infection progresses likely reflects an amplification of this initial effect, possibly driven by viral proteins released during uncoating and/or signaling pathways triggered by infection. Whether stable MTs play a role in later stages of HIV-1 infection is difficult to discern because the virus induces and requires MT stabilization early in its lifecycle. However, expression of Gag polyprotein that is made late in infection also induces MT acetylation, as shown here and in a recent report demonstrating that Gag associates with MTs (Nishi et al., 2009). Notably, interaction of the MA region of Gag with Kif4 regulates Gag intracellular trafficking and production of virus-like particles (VLPs) (Martinez et al., 2008). While this might reflect Kif4's properties as an outward kinesin motor its ability to regulate MT stability, shown here, likely contributes to late stage infection and could explain its positive effects on both early inward and late outward stages of infection.

Our findings demonstrate that an important aspect of early retroviral infection involves the induction of specialized stable MT subsets. We show that the highly specialized host MT end-binding protein, EB1 and its binding partner, Kif4 act as critical host mediators of these events and demonstrate that these poorly understood MT subsets facilitate the delivery of viral particles to the nucleus.

Experimental Procedures

Cells and viruses

293A, 293T and CHME3 cells were described previously (Henning et al., 2010). NHDFs were from Lonza. U87.CD4.CCR5 were from the AIDS Reagent Program (#4035). Jurkats were from ATCC (#TIB-152). Primary monocyte-derived macrophages were prepared as described previously (Jouvenet et al., 2006). HIV-1 based vectors carrying a puromycin resistance gene were produced as described previously (Naghavi et al., 2007). Generation of HIV-1 carrying a luciferase reporter or ZsGreen marker, pNL4-3.Luc.R^-.E^- or pNL4-3.ZsGreen.R^-.E^-, respectively, carrying either CCR5 tropic, VSV-G or MuLV amphotropic envelope glycoprotein is described in Supplemental Information. Vpr labeled viruses were generated similarly by co-transfecting with GFP-Vpr plasmid (McDonald et al., 2002). Mock and non-enveloped virus preparations were generated by transfecting cells without DNA or excluding plasmids for envelope glycoprotein, respectively. 48h post-transfection culture supernatants were harvested, filtered through a 0.45μm filter, concentrated by ultracentrifugation through a 25% sucrose cushion and resuspended in growth medium.

Infections and fusion assays

Cells were infected with different dilutions of HIV-1-VSV-luc or HIV-1-Ampho-luc (1:6000 and 1:2400, respectively), lysed 48-72h.p.i. and assayed for luciferase activity as described (Henning et al., 2010). Infection by puromycin- or neomycin-expressing viruses was measured by colony counting after selection in puromycin (0.5 μg /ml) or geneticin (1 mg/ml). Pseudotyped HIV-1-zsGreen virus was quantified (see supplemental information) and dilutions used such that cells were infected at m.o.i. 3 and 85-95% cells were ZsGreen-positive. An m.o.i. 1 was used for HIV-1-GFP-Vpr infections. Total numbers of viral particles in preparations was estimated by serial dilution of virus and WB analysis of p24 levels against known amounts of purified p24. Virion-based fusion assays were performed as described (Cavrois et al., 2002) with minor modification using ZsGreen-HIV-1-VSV containing the BlaM-Vpr fusion protein (Addgene plasmid 21950). Sample processing is described in Supplemental Information.

RNAi and nocodazole treatment

Cells were transfected on two consecutive days with siRNA duplexes from Ambion; EB1-II (#3891) and EB1-III (#136501), Kif4 (#118455) or control GFP siRNA using RNAiMax (Invitrogen) (Henning et al., 2010). Cells were then seeded, infected and processed as described in the text. For nocodazole experiments cells were rinsed with PBS and growth medium containing nocodazole (Sigma) or DMSO control was added as indicated in the text. Cells were infected with HIV-1-zsGreen for 4h in the presence of nocodazole or DMSO and then medium was replaced with fresh drug-containing medium. 48h.p.i. cultures were harvested, fixed with 4% paraformaldehyde and analyzed by fluorescence-activated cell sorting (FACS) using a Guava easyCyte 8HT Flow Cytometer (EMD Millipore) and FlowJo Software (Treestar).

qPCR measurement of mRNAs and viral DNA

Cytoplasmic RNA was reverse transcribed into cDNA and used as template for PCR (Naghavi et al., 2007). EB1 transcript levels were determined using primers 3 and 9 in Table S1. To quantify viral DNA, cells were infected at high m.o.i. with HIV-1-VSV-puro or HIV-1-Ampho-puro as described (Henning et al., 2010). As negative controls, cells were infected with equal amounts of virus that was heat inactivated at 56°C for 30 min. Hirt DNA was isolated at 24 h.p.i. and the amount of HIV-1 MSS-DNA and total viral DNA was measured using primers specific to MSS and puromycin; copy numbers were interpolated from detection threshold (C_T) values using a full-length HIV-1, pNL4-3 or a puromycin standard curve (Henning et al., 2010).

Antibodies, Western Blotting and Co-IP

Antibodies used were; EB1 (sc-47704) and GAPDH (sc-25778) from Santa Cruz, Flag (F7425), Kif4 (K1765) and acetylated tubulin (T7451) from Sigma, tyrosinated tubulin (ab6160), HIV-1 p24 (ab9071), HIV-1 Gag (ab63917) and GFP (ab13970) from Abcam, detyrosinated tubulin (AB3201) from EMD Millipore, eIF4E (610269) from BD Biosciences, PABP1 (4992) from Cell Signaling Technology. For WB analysis primary antibodies were used at 1:1000 dilution and detected using the appropriate HRP-conjugated secondary. For Co-IP HeLa cells were transfected with HA-tagged forms of Gag, generated as described in Supplemental Information. 48h later soluble cell extracts were prepared as described previously (Henning et al., 2010) and precleared with protein G-sepharose. Input samples were taken and the remainder of the sample was incubated with mouse anti-Kif4 antibody and protein G-sepharose for 2h at 4^0C. Immune complexes were then washed and boiled in Laemmli buffer.

IF and microscopy

Cells were grown on glass coverslips and fixed with ice-cold methanol, then blocked and permeabilized with PBS supplemented with 2% BSA, 10% FBS and 1% Triton X-100. Samples were incubated with primary antibody overnight at 4^0C, washed and incubated with the appropriate AlexaFluor-conjugated secondary for 1h at RT. Images were acquired using a Zeiss LSM 710 confocal laser scanning microscope or motorized spinning-disc confocal microscope (Yokogawa CSU-X1 A1 confocal head and Zeiss Axio Observer Z1 microscope). Orthogonal views were created using Slidebook Three-View. Processing and distance measurements were done using SlideBook software (Intelligent Imaging Innovations). Intensity measurement of stable MTs was done by intensity-based segmentation using the Ridler-Calvard thresholding method. For TIRF microscopy, cells were stained, mounted in TBS and imaged on a Nikon TE2000 microscope with a 60X, 1.45 objective and an Orca II ER CCD (Hamamatsu) camera controlled by MetaMorph software (Wen et al., 2004).

Expression constructs and stable lines

Expression constructs for C-terminally HA-tagged HIV-1 Gag, MA, Gag mutants in MA, and HA-tagged SIV MA are described in Supplemental Information. MoMuLV vectors encoding Flag, EB1-Flag or EB1-C-Flag were generated as described in Supplemental Information and used to infect CHME3 cells. Lines stably expressing Flag, EB1-Flag or EB1-C-Flag were isolated by selection as described (Henning et al., 2010).

Supplementary Material

Refer to Web version on PubMed Central for supplementary material.

Acknowledgments

We thank Thomas Hope, John Moore, Marilyn Resh, Marielle Cavrois and Theodora Hatziioannou for providing reagents and Nagendran Ramalingam and Siddarth Venkatesh for technical help. The following reagent was obtained through the NIH AIDS Research and Reference Reagent Program, Division of AIDS, NIAID, NIH: pNL4-3.Luc.R^-.E^- from Dr. Nathaniel Landau. Y.S. is supported by the Howard Hughes Medical Institute (HHMI). S.P.G. is an Investigator of the HHMI. M.H.N. is a Schaefer Scholar. This study was supported by NIH grant GM101975 and Wellcome Trust grant 085798/Z/08/Z to M.H.N., and NIH grant GM062939 to G.G.G.

References

Arhel N, Genovesio A, Kim KA, Miko S, Perret E, Olivo-Marin JC, Shorte S, Charneau P. Quantitative four-dimensional tracking of cytoplasmic and nuclear HIV-1 complexes. Nature methods. 2006; 3:817–824. [PubMed: 16990814]

Arhel NJ, Souquere-Besse S, Munier S, Souque P, Guadagnini S, Rutherford S, Prevost MC, Allen TD, Charneau P. HIV-1 DNA Flap formation promotes uncoating of the pre-integration complex at the nuclear pore. Embo J. 2007; 26:3025–3037. [PubMed: 17557080]

Bukrinskaya A, Brichacek B, Mann A, Stevenson M. Establishment of a functional human immunodeficiency virus type 1 (HIV-1) reverse transcription complex involves the cytoskeleton. J Exp Med. 1998; 188:2113–2125. [PubMed: 9841925]

Campbell EM, Hope TJ. Gene therapy progress and prospects: viral trafficking during infection. Gene therapy. 2005; 12:1353–1359. [PubMed: 16151445]

Cavrois M, De Noronha C, Greene WC. A sensitive and specific enzyme-based assay detecting HIV-1 virion fusion in primary T lymphocytes. Nat Biotechnol. 2002; 20:1151–1154. [PubMed: 12355096]

Contreras X, Mzoughi O, Gaston F, Peterlin BM, Bahraoui E. Protein kinase C-delta regulates HIV-1 replication at an early post-entry step in macrophages. Retrovirology. 2012; 9:37. [PubMed: 22554282]

Dodding MP, Way M. Coupling viruses to dynein and kinesin-1. Embo J. 2011; 30:3527–3539. [PubMed: 21878994]

Elliott G, O'Hare P. Herpes simplex virus type 1 tegument protein VP22 induces the stabilization and hyperacetylation of microtubules. Journal of virology. 1998; 72:6448–6455. [PubMed: 9658087]

Frampton AR Jr. Uchida H, von Einem J, Goins WF, Grandi P, Cohen JB, Osterrieder N, Glorioso JC. Equine herpesvirus type 1 (EHV-1) utilizes microtubules, dynein, and ROCK1 to productively infect cells. Veterinary microbiology. 2010; 141:12–21. [PubMed: 19713056]

Gallo DE, Hope TJ. Knockdown of MAP4 and DNAL1 produces a post-fusion and pre-nuclear translocation impairment in HIV-1 replication. Virology. 2012; 422:13–21. [PubMed: 22018492]

Gouveia SM, Akhmanova A. Cell and molecular biology of microtubule plus end tracking proteins: end binding proteins and their partners. International review of cell and molecular biology. 2010; 285:1–74. [PubMed: 21035097]

Haedicke J, de Los Santos K, Goff SP, Naghavi MH. The Ezrin-radixin-moesin family member ezrin regulates stable microtubule formation and retroviral infection. Journal of virology. 2008; 82:4665–4670. [PubMed: 18305045]

Henning MS, Morham SG, Goff SP, Naghavi MH. PDZD8 is a novel Gag-interacting factor that promotes retroviral infection. Journal of virology. 2010; 84:8990–8995. [PubMed: 20573829]

Henning MS, Stiedl P, Barry DS, McMahon R, Morham SG, Walsh D, Naghavi MH. PDZD8 is a novel moesin-interacting cytoskeletal regulatory protein that supresses infection by herpes simplex virus type 1. Virology. 2011 In Press.

Hulme AE, Perez O, Hope TJ. Complementary assays reveal a relationship between HIV-1 uncoating and reverse transcription. Proceedings of the National Academy of Sciences of the United States of America. 2011; 108:9975–9980. [PubMed: 21628558]

Husain M, Harrod KS. Enhanced acetylation of alpha-tubulin in influenza A virus infected epithelial cells. FEBS letters. 2011; 585:128–132. [PubMed: 21094644]

Janke C, Bulinski JC. Post-translational regulation of the microtubule cytoskeleton: mechanisms and functions. Nat Rev Mol Cell Biol. 2011; 12:773–786. [PubMed: 22086369]

Jouvenet N, Monaghan P, Way M, Wileman T. Transport of African swine fever virus from assembly sites to the plasma membrane is dependent on microtubules and conventional kinesin. Journal of virology. 2004; 78:7990–8001. [PubMed: 15254171]

Jouvenet N, Neil SJ, Bess C, Johnson MC, Virgen CA, Simon SM, Bieniasz PD. Plasma membrane is the site of productive HIV-1 particle assembly. PLoS biology. 2006; 4:e435. [PubMed: 17147474]

Kannan H, Fan S, Patel D, Bossis I, Zhang YJ. The hepatitis E virus open reading frame 3 product interacts with microtubules and interferes with their dynamics. Journal of virology. 2009; 83:6375–6382. [PubMed: 19369329]

Kim W, Tang Y, Okada Y, Torrey TA, Chattopadhyay SK, Pfleiderer M, Falkner FG, Dorner F, Choi W, Hirokawa N, Morse HC 3rd. Binding of murine leukemia virus Gag polyproteins to KIF4, a microtubule-based motor protein. Journal of virology. 1998; 72:6898–6901. [PubMed: 9658142]

Leung J, Yueh A, Appah FS Jr. Yuan B, de los Santos K, Goff SP. Interaction of Moloney murine leukemia virus matrix protein with IQGAP. Embo J. 2006; 25:2155–2166. [PubMed: 16628219]

Li R, Gundersen GG. Beyond polymer polarity: how the cytoskeleton builds a polarized cell. Nat Rev Mol Cell Biol. 2008; 9:860–873. [PubMed: 18946475]

Martinez NW, Xue X, Berro RG, Kreitzer G, Resh MD. Kinesin KIF4 regulates intracellular trafficking and stability of the human immunodeficiency virus type 1 Gag polyprotein. Journal of virology. 2008; 82:9937–9950. [PubMed: 18684836]

McDonald D, Vodicka MA, Lucero G, Svitkina TM, Borisy GG, Emerman M, Hope TJ. Visualization of the intracellular behavior of HIV in living cells. J Cell Biol. 2002; 159:441–452. [PubMed: 12417576]

Miyauchi K, Kim Y, Latinovic O, Morozov V, Melikyan G. HIV enters cells via endocytosis and dynamin-dependent fusion with endosomes. Cell. 2009; 137:433–444. [PubMed: 19410541]

Naghavi MH, Goff SP. Retroviral proteins that interact with the host cell cytoskeleton. Current opinion in immunology. 2007; 19:402–407. [PubMed: 17707624]

Naghavi MH, Valente S, Hatziioannou T, de Los Santos K, Wen Y, Mott C, Gundersen GG, Goff SP. Moesin regulates stable microtubule formation and limits retroviral infection in cultured cells. Embo J. 2007; 26:41–52. [PubMed: 17170707]

Naranatt PP, Krishnan HH, Smith MS, Chandran B. Kaposi's sarcoma-associated herpesvirus modulates microtubule dynamics via RhoA-GTP-diaphanous 2 signaling and utilizes the dynein motors to deliver its DNA to the nucleus. Journal of virology. 2005; 79:1191–1206. [PubMed: 15613346]

Nishi M, Ryo A, Tsurutani N, Ohba K, Sawasaki T, Morishita R, Perrem K, Aoki I, Morikawa Y, Yamamoto N. Requirement for microtubule integrity in the SOCS1-mediated intracellular dynamics of HIV-1 Gag. FEBS letters. 2009; 583:1243–1250. [PubMed: 19327355]

Parker JS, Broering TJ, Kim J, Higgins DE, Nibert ML. Reovirus core protein mu2 determines the filamentous morphology of viral inclusion bodies by interacting with and stabilizing microtubules. Journal of virology. 2002; 76:4483–4496. [PubMed: 11932414]

Petit C, Giron ML, Tobaly-Tapiero J, Bittoun P, Real E, Jacob Y, Tordo N, De The H, Saib A. Targeting of incoming retroviral Gag to the centrosome involves a direct interaction with the dynein light chain 8. J Cell Sci. 2003; 116:3433–3442. [PubMed: 12857789]

Su Y, Qiao W, Guo T, Tan J, Li Z, Chen Y, Li X, Li Y, Zhou J, Chen Q. Microtubule-dependent retrograde transport of bovine immunodeficiency virus. Cell Microbiol. 2010; 12:1098–1107. [PubMed: 20148896]

Tang Y, Winkler U, Freed EO, Torrey TA, Kim W, Li H, Goff SP, Morse HC 3rd. Cellular motor protein KIF-4 associates with retroviral Gag. Journal of virology. 1999; 73:10508–10513. [PubMed: 10559369]

Valenzuela-Fernandez A, Alvarez S, Gordon-Alonso M, Barrero M, Ursa A, Cabrero JR, Fernandez G, Naranjo-Suarez S, Yanez-Mo M, Serrador JM, et al. Histone deacetylase 6 regulates human immunodeficiency virus type 1 infection. Mol Biol Cell. 2005; 16:5445–5454. [PubMed: 16148047]

Warren JC, Cassimeris L. The contributions of microtubule stability and dynamic instability to adenovirus nuclear localization efficiency. Cell Motil Cytoskeleton. 2007; 64:675–689. [PubMed: 17565754]

Wen Y, Eng CH, Schmoranzer J, Cabrera-Poch N, Morris EJ, Chen M, Wallar BJ, Alberts AS, Gundersen GG. EB1 and APC bind to mDia to stabilize microtubules downstream of Rho and promote cell migration. Nat Cell Biol. 2004; 6:820–830. [PubMed: 15311282]

Yea C, Dembowy J, Pacione L, Brown M. Microtubule-mediated and microtubule-independent transport of adenovirus type 5 in HEK293 cells. Journal of virology. 2007; 81:6899–6908. [PubMed: 17442712]

Yoder A, Guo J, Yu D, Cui Z, Zhang XE, Wu Y. Effects of microtubule modulators on HIV-1 infection of transformed and resting CD4 T cells. Journal of virology. 2011; 85:3020–3024. [PubMed: 21209111]

Highlights

- HIV-1 induces microtubule (MT) stabilization to facilitate early infection
- EB1 is a critical host regulator of MT stabilization and viral infection
- Kif4 binds EB1 and mediates MT stabilization by the HIV-1 matrix protein

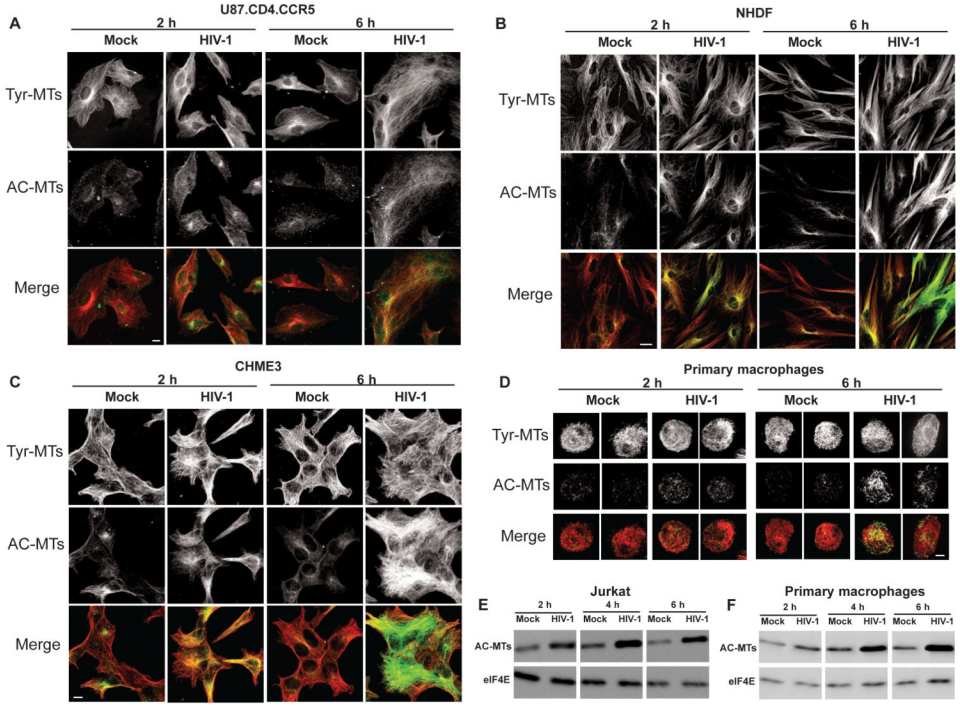

Figure 1. HIV-1 induces acetylated MT formation in human cells

(A-D) Cells were infected with HIV-1 then samples were fixed at the indicated h.p.i. and stained for Tyr-MTs and AC-MTs. U87.CD4.CCR5 cells were mock infected or infected at m.o.i. 3 with HIV-1 carrying HIV-1 envelope (A); NHDFs (B), CHME3 cells (C) or primary human macrophages (D) were mock infected or infected with HIV-1-VSV. Images are shown for representative time points of 2h.p.i. and 6h.p.i. Scale bar, 10μm. (E-F) WB analysis of AC-MT levels in mock infected and HIV-1-VSV infected jurkat cells (E) and primary human macrophages (F) at the indicated h.p.i. eIF4E was used as loading control. See also Figure S1.

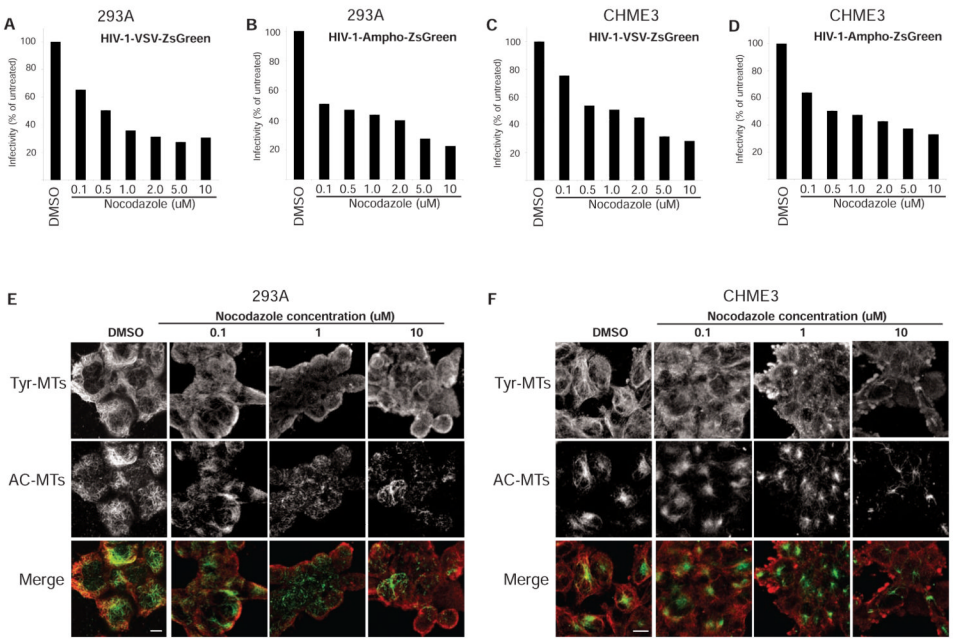

Figure 2. Nocodazole depolymerizes dynamic MTs and modestly reduces infection by HIV-1

293A (A and B) or CHME3 (C and D) cells were treated for 1 h with either DMSO or increasing concentrations of nocodazole (0.1-10 μM). Cells were infected at m.o.i. 3 with HIV-1-VSV-ZsGreen (A and C) or HIV-1-Ampho-ZsGreen (B and D) followed by FACS analysis of ZsGreen positive cells. Nocodazole-treated samples were normalized to DMSO treated negative controls to determine % infectivity. (E and F) DMSO- or nocodazole-treated 293A (E) or CHME3 (F) as in A-D were fixed and stained for Tyr-MTs and AC-MTs 1 h post-treatment. Images are shown for representative nocodazole concentrations as indicated. Scale bar, 10 μm.

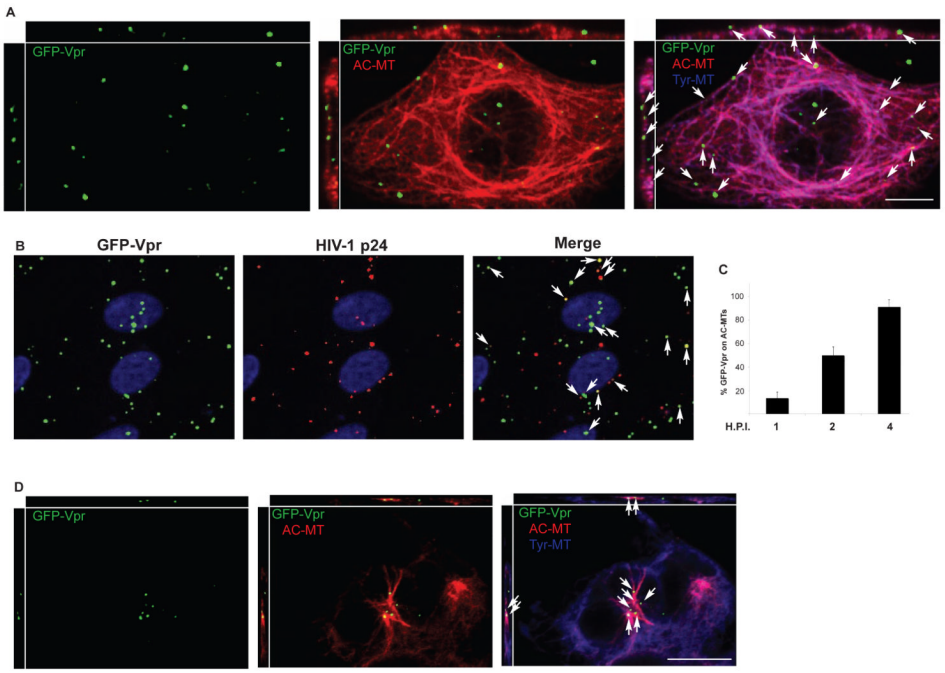

Figure 3. HIV-1 localizes to stable MTs in the presence of nocodazole

(A) CHME3 cells were infected with HIV-1-VSV-GFP-Vpr at m.o.i. 1 for 4h. Cultures were fixed and stained for Tyr-MTs (blue), AC-MTs (red) and GFP (green). Arrows point to viral particles localized to AC MT networks. Orthogonal views are presented above and to the left of each regular imaging plane (top *x-z*, left *z-y*), scale bar, 10μm. (B) Cells were infected with HIV-1-VSV-GFP-Vpr for 2h then fixed and stained for GFP and HIV-1 p24. Arrows point to representative viral particles that co-stain for both proteins. (C) Quantification of the % viral particles associated with AC MTs represented as mean +/− SEM at 1, 2 and 4h.p.i. in CHME3 cells infected as in A. (D) CHME3 cells were treated with 0.25 μM nocodazole for 20 min then infected for 1h with HIV-1-VSV-GFP-Vpr and processed as in A. Arrows indicate the localization of virions to AC-MTs. Scale bar, 10μm.

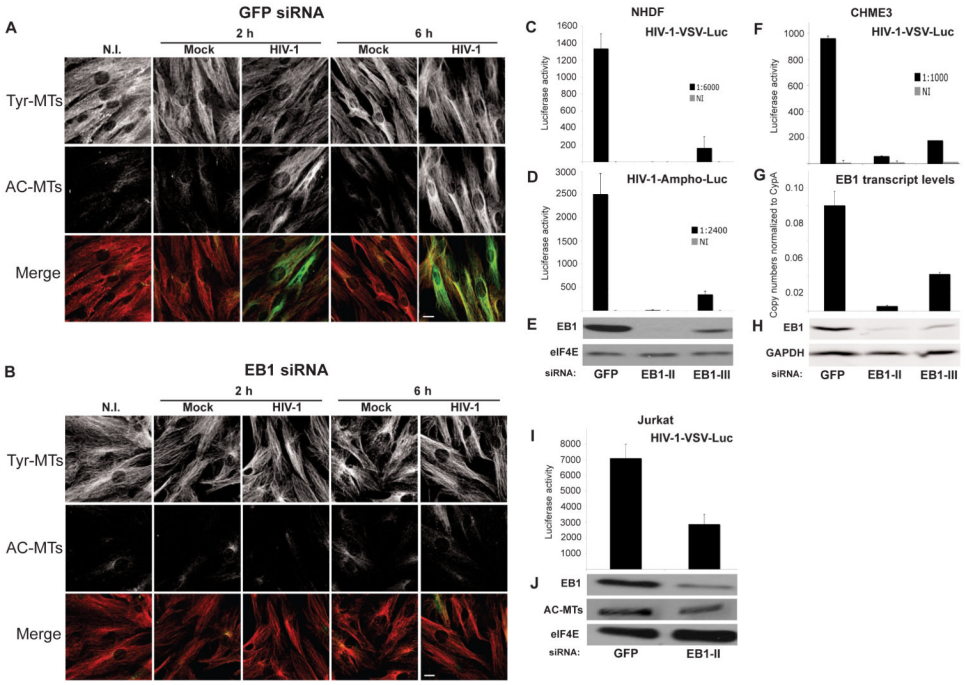

Figure 4. EB1 is required for HIV-1 mediated MT stabilization and infection

(A-B) NHDFs were transfected with control GFP siRNA (A) or EB1 siRNA (B) and then non-infected (N.I.), mock infected or infected with HIV-1-VSV at m.o.i. 3. Samples were fixed at the indicated h.p.i. and stained for Tyr-MTs and AC-MTs. Images are shown for representative fields. Scale bar, 10 μm. (C-E) NHDFs were transfected with control GFP siRNA or two independent EB1 siRNAs (EB1-II and EB1-III) and then infected with HIV-1-VSV-Luc (C) or HIV-1-Ampho-Luc (D). Levels of infection were determined by luciferase assay. (E) WB analysis demonstrated the extent of EB1 depletion in samples. eIF4E served as a loading control. (F-H) CHME3 cells were transfected with control, EB1-II or EB1-III siRNAs and then infected with HIV-1-VSV-Luc. (F) Luciferase assays were used to determine levels of infection. (G) qPCR showing EB1 transcript levels in each sample. (H) WB analysis of EB1 depletion in samples. GAPDH served as a loading control. (I-J) Jurkat cells were treated with control or EB1-II siRNAs and infected with HIV-1-VSV-Luc. (I) Luciferase assays were used to determine levels of infection. (J) WB analysis of EB1 depletion and AC-MTs in samples. eIF4E was used as loading control. Data in C, D, F, G and I are represented as mean +/− SEM. See also Figure S2.

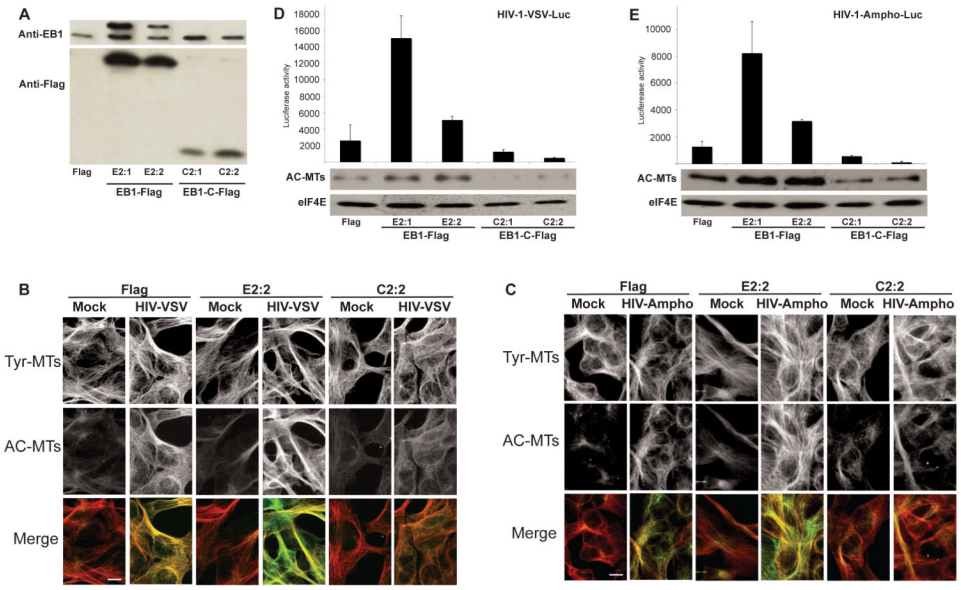

Figure 5. Stable expression of a dominant negative carboxy-terminal fragment of EB1 inhibits MT stabilization and HIV-1 infection in CHME3 cells

(A) WB analysis of EB1 (upper panel) or transgene EB1 (lower panel) levels in CHME3 cells stably expressing control Flag, EB1-Flag or dominant negative EB1-C-Flag using anti-EB1 or anti-Flag antibodies. (B-C) IF analysis of Tyr-MTs and AC-MTs in representative clones of Flag, EB1-Flag (E2:2) or EB1-C-Flag (C2:2) either mock infected or infected at m.o.i. 3 with HIV-1-VSV (B) or HIV-1-Ampho (C). Cultures were fixed and stained for Tyr-MTs and AC-MTs at 6 h.p.i. Scale bar, 10μm. (D-E) Flag, EB1-Flag or EB1-C-Flag clones were infected with HIV-1-VSV-luc (D) or HIV-1-Ampho luc (E) followed by the measurement of luciferase activity 48 h.p.i. to determine levels of infection (upper panels). Data are represented as mean +/− SEM. Stable MT levels in infected clones 6 h.p.i. were determined by WB using anti-acetylated tubulin antibody (AC-MTs) (middle panels). eIF4E served as a loading control (lower panels).

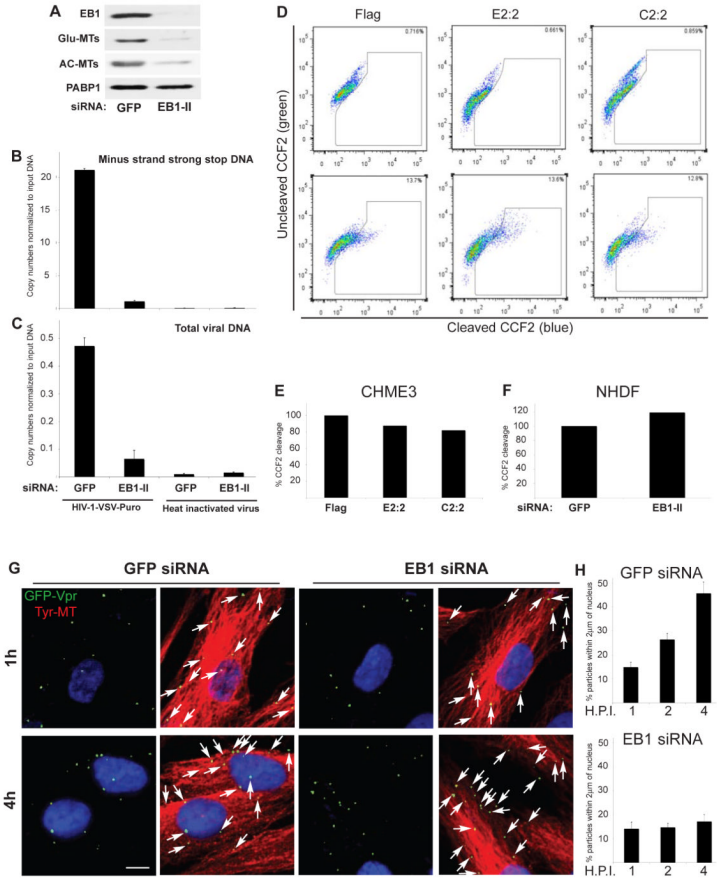

Figure 6. EB1 promotes an early post-fusion stage of HIV-1 infection

(A-C) Effects of EB1 depletion on HIV-1 DNA synthesis. CHME3 cells were transfected with control GFP siRNA or EB1 siRNA (EB1-II). (A) 24h post-transfection cells were lysed and analyzed by WB using antibodies to EB1, Glu-MTs, AC-MTs or PABP1 (as loading control). (B-C) 24h post-transfection cells were infected with HIV-1-VSV-puro. Low molecular Hirt DNA was isolated at 24 h.p.i. and levels of viral MSS-DNA (B) and total viral DNA (C) in samples were measured by qPCR using primers specific to MSS and puromycin, respectively. Copy numbers were calculated and normalized to input DNA in each sample. Data are represented as mean +/− SEM. (D-F) Effects of EB1 on fusion of HIV-1 cores into the cytosol. (D-E) CHME3 cells expressing Flag, EB1-Flag (E2:2) or EB1-C-Flag (C2:2) were either mock infected (upper panels) or infected with HIV-1-VSV-ZsGreen containing BlaM-Vpr (lower panels). (D) FACS analysis of cells infected at high m.o.i. showing ~13% shift from green (uncleaved CCF2) to blue (cleaved CCF2) cells in Flag, E2:2 and C2:2 clones. (E) Quantification of the effects of E2:2 and C2:2 on HIV-1 fusion at low m.o.i. using the BlaM-Vpr assay, normalized to control Flag lines. (F) NHDFs were treated with control GFP or EB1 siRNAs then infected at low m.o.i. with HIV-1-VSV-ZsGreen containing BlaM-Vpr. Samples were analyzed by FACS and effects of EB1 depletion on HIV-1 fusion were normalized to control siRNA-treated samples. (G-H) EB1 depletion inhibits the translocation of viral particles across the cytoplasm to the nucleus. NHDFs were treated with control GFP or EB1 siRNAs then infected with HIV-1-VSV-GFP-Vpr at m.o.i. 1. (G) After 1h or 4h samples were fixed and stained for Tyr-MTs and GFP. Nuclei were stained with DAPI. Representative images are shown. Scale bar, 10μm. (H)

Quantification of the percentage of virions within 2μm of the nucleus in infected cells at 1h, 2h or 4h represented as mean +/− SEM. n≤36 cells and n>400 viral particles per sample. See also Figure S3.

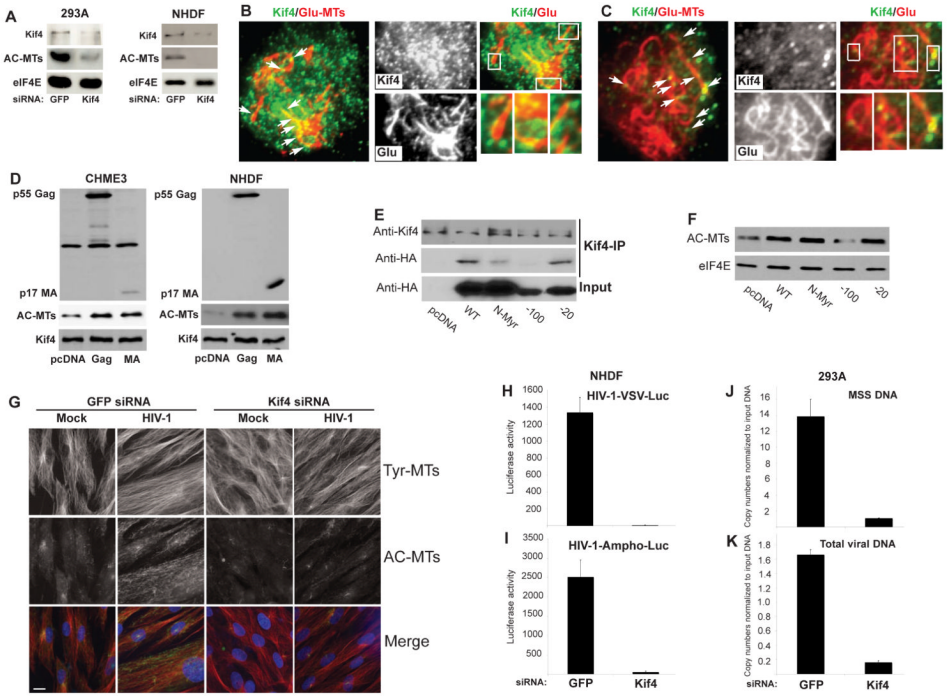

Figure 7. Kif4 mediates MT stabilization and early HIV-1infection

(A) Kif4 regulates AC MT levels in human cells. 293A or NHDF cells were transfected with control or Kif4 siRNAs then analyzed by WB with the indicated antibodies. (B-C) TIRF microscopy images of infected 293A (B) and CHME3 cells (C). Cells were infected with HIV-1-VSV then fixed and stained for Kif4 and Glu-MTs. Kif4 present on Glu-MTs at the periphery of HIV-1 infected cells is indicated by arrows. (B-C, right panels) Higher magnification images of Kif4 on Glu-MTs from samples in B and C. Boxed regions in the merged image are shown at higher magnification in the lower right panels. (D) Expression of Gag or MA induces MT acetylation in human cells. CHME3 or NHDF cells were transfected with control pcDNA, pcDNA-Gag or pcDNA-MA then analyzed by WB using anti-HIV-1 Gag, anti-Kif4 and anti-AC-tubulin antibodies. (E-F) An N-terminal region of HIV-1 MA mediates binding to Kif4 and MT stabilization. (E) HeLa cells were transfected with HA-tagged forms of Gag and immunoprecipitated using anti-Kif4 antibody. WB using anti-Kif4 or anti-HA antibodies shows the levels of Kif4 or HIV-1 Gag polyprotein in immune complexes and input levels of Gag. (F) WB analysis of AC-MT levels in HeLa cells 48h after transfection with HA-tagged forms of Gag. eIF4E served as loading control. (G) Kif4 is required for HIV-1-induced MT stabilization. NHDF cells were transfected with control or Kif4 siRNAs then infected with HIV-1-VSV for 6h. Fixed samples were stained for AC-MTs (green) and Tyr-MTs (red). Nuclei were stained with Hoechst. Scale bar, 10μm. (H-I) Kif4 is required for HIV-1 infection. NHDFs were transfected with control or Kif4 siRNAs then infected with HIV-1-VSV-luc (H) or HIV-1-Ampho-luc (I). Infectivity was determined by measurement of luciferase activity 48 h.p.i. (J-K) Effects of Kif4 depletion on HIV-1 DNA synthesis. Control or Kif4 siRNA treated cells were infected with HIV-1-VSV-puro and levels of viral MSS-DNA (J) and total viral DNA (K) in samples were measured by qPCR. Data in H-K are represented as mean +/− SEM. See also Figure S4.